Chemical Methodologies 6(2022) 962-976

Chemical Methodologies

Journal homepage: http://chemmethod.com

Original Research Article

Synthesis, Characterization, and Biological Activity of Mixed Ligand Complexes from 8-Hydroxyquinoline and New Ligand for *β*-Enaminone

Maysam B. Abdulsalam, Ahmed T. Numan*

Department of Chemistry, College of Education for Pure Sciences, Ibn-Al-Haitham, University of Baghdad, Baghdad, Iraq

ARTICLE INFO

Article history

Submitted: 2022-06-16
Revised: 2022-07-28
Accepted: 2022-09-11
Manuscript ID: CHEMM-2208-1593
Checked for Plagiarism: Yes
Language Editor:
Dr. Nadereh Shirvani
Editor who approved publication:
Dr. Lotfali Saghatforoush

DOI:10.22034/CHEMM.2022.356340.1593

KEYWORDS

β-Enaminones
5,5-Dimethylcyclohexane-1,3-dione
Furosemide
Mixed-ligand complexes
8-Hydroxyquinoline

ABSTRACT

[4-Chloro-5-(*N*-(5,5-dimethyl-3-oxocyclohex-1-en-1-yl) sulfamoyl)-2-((furan-2-ylmethyl) amino) benzoic acid] is the ligand[H_2L_1]. [H_2L_1] was synthesized and identified using Fourier transform infrared (FT-IR), ^{1}H, ^{13}C-NMR, CHN, mass spectra, and UV-Vis spectroscopy methods. To detect mixed ligand complexes, analytical and spectroscopic approaches such as micro-analysis, conductance, UV-visible, magnetic susceptibility, and FT-IR spectra were utilized. Its mixed ligand complexes [M(L_1) (Q)Cl_2] and complexes [Pd(L_1) (Q)] and [Pt(L_1) (Q)Cl_2]; [H_2L_1] = *β*-enaminone ligand =L_1 and Q= 8-Hydroxyquinoline = L_2]. The results showed that the complexes were synthesized utilizing the molar ratio M: L_1:L_2 (1:1:1). For the metal complexes Co(II), Ni(II), Cd(II), and Pt(IIII), a six-coordinate octahedral geometry was proposed, whereas the Pd(II) complex was square planar. By Using the agar well diffusion method, the ligands and complexes were evaluated for antibacterial activity against *Staphylococcus aureus* and *Escherichia coli*. The studies demonstrate that the ligand and its complexes have variable activity against the bacterial types. Some of the complexes had an effect on affected bacteria, while others had less inhibitory action than the ligand. Also, the produced ligand and its metal complexes have been tested for fungi (*Candida albicans*); the complexes exhibited suppressing activity against fungi compared to the ligand prepared from them.

GRAPHICAL ABSTRACT

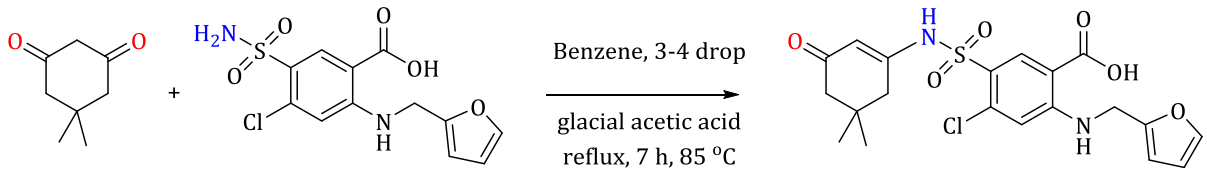

[4-Chloro-5-(N-(5,5-dimethyl-3-oxocyclohex-1-en-1-yl) sulfamoyl)-2-((furan-2-ylmethyl) amino) benzoic acid] = [H_2L_1]

* Corresponding author: Ahmed T. Numan
✉ E-mail: ahmed.t.n@ihcoedu.uobaghdad.edu.iq

Introduction

Enaminones have received great attention in organic synthesis due to their importance as precursors for developing several bioactive heterocyclic compounds. Due to the presence of both electrophilic and nucleophilic sites in its structure, enaminone derivatives have a wide range of applications as intermediates [1]; therefore, they have also been made used as starting materials for the synthesis of anti-inflammatory, antibacterial, anticonvulsant, and antitumor agents [2], as well as in the production of naturally occurring alkaloids. The significant advantages of enaminone derivatives are their stability under simulated physiological pH conditions and low levels of toxicity [3]. The conjugated system of *β*-enaminone function is a functional group in the drug industry. Enaminones produced from *β*-carbonyl molecules are relatively stable, most likely owing to keto-enol and imine-enamine tautomeric equilibrium (Scheme 1) [4]. Notably, molecule's structure shows a strong intramolecular hydrogen bond along the heterodienic O=C–C=C–NH moiety, which takes the shape of a six-membered ring and makes the structure stiffer [5].

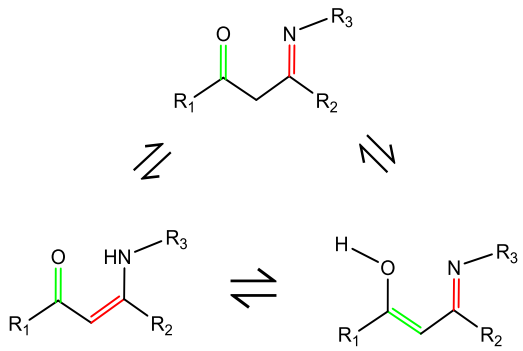

Scheme 1: Tautomeric equilibria of β-enaminones

5,5-dimethylcyclohexane-1,3-dione is an organic compound that belongs to the cyclic *ß*-diketones type [6]. These white to light yellow crystallines are also known as dimedone, methone, dimethyldihydro resorcinol and cyclomethone. The melting point of $C_8H_{12}O_2$ (M.wt = 140.179 g/mol) is 147-150 °C (420-423 K). It is stable in ambient conditions and soluble ethanol, methanol, and water, as well as inorganic solvents [6-8]. It is one of the most prominent cyclic 1,3-dicarbonyls, and its uses may be found in a variety of various fields, including industrial, synthetic organic chemistry, and analytical chemistry [9].

Furosemide chemical name is 4-chloro-2-[(2-furanylmethyl)-amino]-5-sulfamoylbenzoic acid [10, 11]. It is known by the generic names Furosemide and Lasix [12]. It is a loop diuretic with a high ceiling that is used to treat edema and hypertension associated with congestive heart failure, renal disease, and cirrhosis of the liver liver cirrhosis [13, 14]. Its molecule includes potential hydrogen bond donor and acceptor groups: $-SO_2NH_2$, NH, and COOH [15].

The mixed ligand may play an essential part in the biological sector, as seen by the numerous different ways that enzymes are known to be activated by metal ions [16]. N- and O- donor ligands were utilized in the production of metal complexes to study a variety of antifungal and antimicrobial activities [17]. Organic bi-dentate ligands have been the most important class of ligands in coordination chemistry, and they have numerous applications in various fields. The ligands are composed of donor atoms, such as nitrogen, oxygen, and carbonyl groups. Consequently, its own interaction with metal ions results in the formation of complexes with different geometries that are biologically active. In latest years, mixed ligand transition metal complexes have gained prominence. These complexes have been studied for their utility in various fields. Some metal-ligand complexes catalyzed oxidation, oxidative cleavage, reduction, etc. [18, 19]. It is well established that mixed ligand chelates play an important essential role in biological processes such as the activation of activating enzymes, storage and transport of and storing and transporting substances across membranes [20].

8-Hydroxyquinoline is a white to off-white crystal or powder that is insoluble in water but freely soluble in aqueous mineral acids, acetone, ethanol, and chloroform [21]. The chemical compound 8-Hydroxyquinoline (8-HQ, 8-quinolinol, C_9H_7NO, oxine) [22] is a small, bicyclic compound widely used in medicinal chemistry,

analytical chemistry, nuclear medicine, and as an imaging agent in nuclear medicine.

Numerous applications exist for the 8-HQ molecule; In medicine, 8-HQ and its derivatives are utilized as antimicrobials, anticancer properties, and anti-neurodegeneration. Whilst While in agriculture, they are employed as fungicides and insecticides [23, 24].

J. Shashikanth *et. al*. [25] collection of reactions to produce β-enaminones was successfully done using 5,5-dimethyl-1,3-cyclohexanedione, amines, and BiOCl fakes as catalysts enhanced by visible light. The produced BiOCl fakes were characterized using a variety of various analytical techniques and examined for photo-catalytic application using methylene blue dye under a variety of various experimental conditions. The uses of 5,5-dimethyl-1,3-cyclohexanedione to synthesize *β*-enaminones and their derivatives in the presence of visible light irradiation. The method utilized to prepare the photocatalyst is easily scaled up for bulk as it consumes a maximum of 10 min. additionally, it reduces costs because no sophisticated equipment is required, Scheme 2.

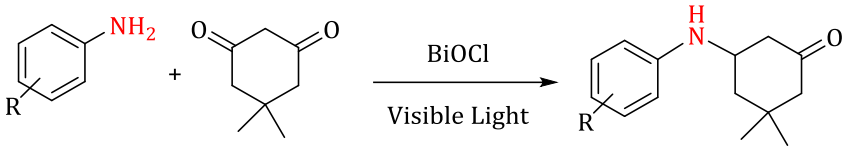

Scheme 2: Synthesis *β*-enaminone by using BiOCl fakes as the catalyst

Hassan J. Kadhom *et al*. [26] created *β*-enaminones and their complexes. Approximately 63% of the ligands were synthesized from amines (pyrimidine-2,4-diamine) and 1,3-dicarbonyl compounds (dimedone). Its mixed ligand complexes (ML_13ph) [M = Co(II), Ni(II), Cu(II), Zn(II), and Cd(II); (H_1L_1) = *β*-enaminone ligand=L_1 and (3ph) = 3-aminophenol=L_2]. Results indicate that complexes are formed with a molar ratio of M: L_1:L_2 (1:1:1). To form a suitable complex, a tetradentate *β*-enaminone ligand with N_3O donor atoms is coordinated to Co(II), Ni(II), Cu(II), Zn(II), and Cd(II) ions. The antifungal and antibacterial properties of the synthesized ligand and its mixed ligand complexes have been evaluated against various pathogenic fungi and bacteria. Compared to the standard antibiotic ciprofloxacin, the biological activity of these compounds was superior.

In this study, attempts were made to synthesize Co(II), Ni(II), Pd(II), Cd(II), and Pt(IIII) mixed ligand complexes of ligand [H_2L_1] and 8-Hydroxyquinoline. All complexes were characterized utilizing spectroscopic techniques, and their biological activity was studied.

Materials and Methods

Every chemical was analytical grade and had not been further purified before usage.

Analytical and physical measurements

Shimadzu (FT-IR)-8300 Infrared Spectrophotometer was used to record FT-IR spectra in the (4000–400) cm^{-1} range. Spectra were recorded on potassium bromide (KBr) discs and Csl discs in the 400-200 cm^{-1} registered on Shimadzu 8400s FT-IR. The Electro-thermal Stuart (SMP40) was utilized for melting point measurement. Electronic spectra were recorded from (200-1100 nm) for 10^{-3} M solutions in DMSO at room temperature using a Shimadzu 1800 (UV-Vis) spectrophotometer with a quartz cell of 1.00 cm in length. Microanalysis (CHN) analyzer on a Heraeus instrument (Vario EL) was used to measure elemental microanalyses. The amount of chloride present in complexes was measured using a potentiometric titration technique using a (686-Titro Processor-665. Dosimat Metrohm Swiss). Magnetic moments (μ_{eff} BM) were determined utilizing a magnetic susceptibility balance (Sherwood-Scientific). The ^{1}H-NMR spectra of the ligands were determined in DMSO-d_6 as a solvent, Utilizing tetramethyl silane (TMS) as an internal standard on Agilent technologies-500 MHz spectrometer. Chemical shifts are measured in ppm downfield from the TMS reference. Electrospray mass spectroscopy was utilized to determine the ligands in the

positive mode on the Agilent Sciex ESI-MS. The metal ratios of the complexes were determined with the help of the atomic absorption (AA) technique. This was done with an atomic absorption spectrophotometer made by Shimadzu (model AA 680 GBC 933 plus).

Synthesis of the ligand [H_2L_1]

A 5,5-dimethyl cyclohexane-1,3-dione (0.105 g, 0.749 moles) was dissolved in absolute benzene 10 mL with a few drops of glacial acetic acid with constant, furosemide (0.25 g, 0.75 mmole) dissolved in 25 mL absolute benzene with a few drops of DMSO were added with continual stirring. The solutions were mixed in a round bottom flask 100 mL, the mixture was then stirred continuously until it converted into a light-yellow solution. The resulting solution was refluxed for 7 hours until the light-yellow precipitate was noted, TLC was used to monitor the reaction. At room temperature, the reaction mixture was allowed to cool. The light-yellow precipitate had a weight of 0.27 g, Yield = % 79.4, m.p = 162 °C, Scheme 3.

Synthesis of mixed ligand metal complexes

The metal solution of $CoCl_2.6H_2O$ (0.078 g, 0.33 mmole) in 5 mL of ethanol was stirred for 10 minutes. The ligand solution [H_2L_1] (0.15 g, 0.33 mmole) in 15 mL of ethanol after being adjusted to pH = 8 utilizing a few drops of potassium hydroxide solution was added to the metal solution. In addition, 8-Hydroxyquinoline (0.0479 g, 0.33 mmole) in 5 mL of ethanol was added to the metal solution described above. The resultant mixture was heated for 4 hours under reflux conditions. A solid complex was formed; It was collected by filtration and dried for 24 hours at ambient temperature. An olive solid was obtained. Weight (0.19 g), Yield = (70.3 %), m.p = >270 °C. The method utilized to prepare the complexes of Ni(II), Cd(II), Pd(II), and Pt(IIII) ions was a similar approach to that described in the section on the preparation of the Co(II) complex (Scheme 4). The micro-analysis of results and a few physical characteristics for ligand(H_2L_1) and the prepared complexes are in Table 1.

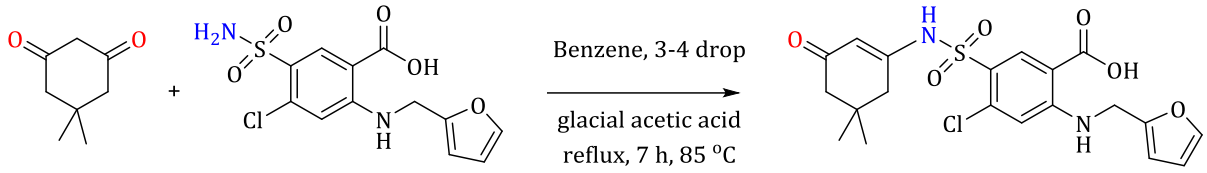

[4-Chloro-5-(N-(5,5-dimethyl-3-oxocyclohex-1-en-1-yl) sulfamoyl)-2-((furan-2-ylmethyl) amino) benzoic acid] = [H_2L_1]

Scheme 3: Synthetic route for the ligand [H_2L_1]

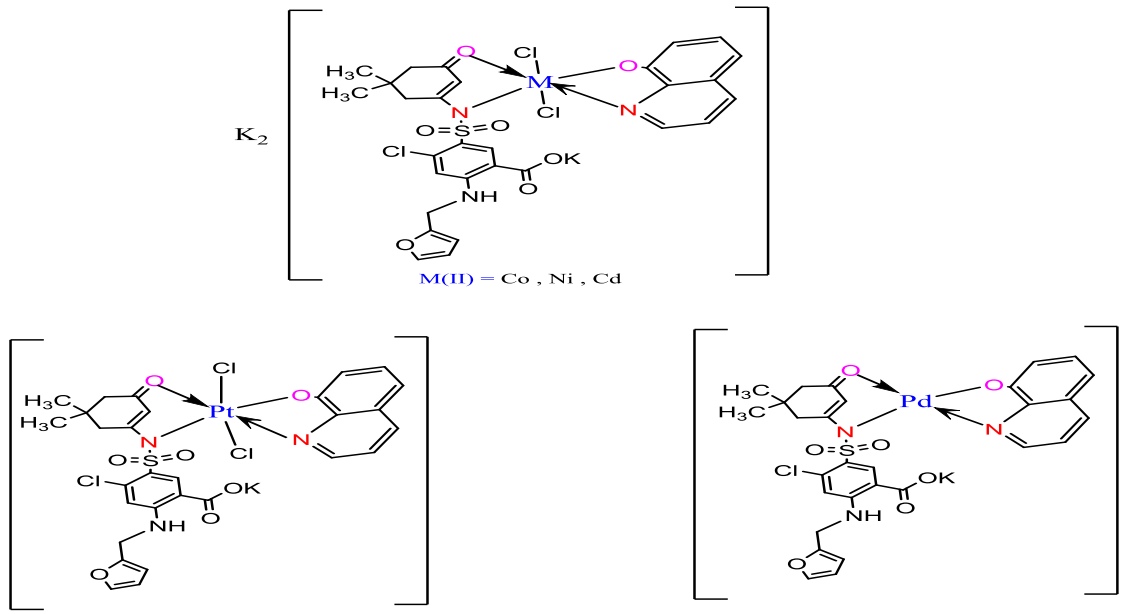

Scheme 4: The suggested chemical structure of the complexes

Table 1: Elemental analysis information and some physical properties for ligand (H_2L_1) and the prepared complexes

No.	Compounds	Color	M.P (°C)	M.Wt g.mol^{-1}	Yield (%)	Elemental analysis found (Calc.)				Molar conductivity (S.cm^2 molar $^{-1}$)
						C	H	N	M	
1	$[H_2L_1]$	Light yellow	162	452.9	79.4	53.04 52.84	4.67 4.46	6.19 6.39	- -	-
2	$K_2[Co(L_1)(Q)Cl_2]$	Olive	>270	842.2	70.3	41.36 41.73	2.99 3.18	4.99 4.81	6.99 7.37	9.59
3	$K_2[Ni(L_1)(Q)Cl_2]$	Pale Green	>270	841.9	82.01	41.36 40.91	2.99 2.65	4.99 4.78	6.96 6.54	11.17
4	K_2 $[Cd(L_1)(Q)Cl_2]$	Yellow	>270	895.7	60.81	38.89 39.02	2.81 2.66	4.69 4.3	12.55 12.73	4.09
5	$[Pd(L_1)(Q)]$	Brown	>270	740.6	66.93	47.03 47.5	3.40 3.88	5.67 5.24	14.37 13.58	16.12
6	$[Pt(L_1)(Q)Cl_2]$	Olive	220*	900.1	59.73	38.70 39.1	2.80 2.63	4.67 4.22	21.65 22.39	12.32

Results and Discussion

*FT- IR Spectral data for ligand $[H_2L_1]$, 8-HQ and $K_2[Co(L_1)(Q)Cl_2]$ (**1**), $K_2[Ni(L_1)(Q)Cl_2]$ (**2**), $[Pd(L_1)(Q)]$ (**3**), $K_2[Cd(L_1)(Q)Cl_2]$ (**4**) and $[Pt(L_1)(Q)Cl_2]$ (**5**) complexes*

As shown in Figure S1 (Supporting information), the N-H stretching vibration is responsible for the sharp band at 3375 cm^{-1}, and the N-H enaminone is responsible for the band at 3251 cm^{-1} and υ OH is responsible for the stretching band at 3498 cm^{-1}. It was determined that the υ C-H aromatic stretching vibrations were responsible for the band at 3082 cm^{-1}. The stretching band υ C-H aliphatic is responsible for the bands detected at 2958 cm^{-1} and 2873 cm^{-1}. The bands at 1681 cm^{-1} and 1616 cm^{-1} were attributed to C=O ketone and C=O stretching vibrations respectively. The stretching bands υ asymmetric S=O and υ symmetric S=O are responsible for the bands detected at 1346 cm^{-1} and 1165 cm^{-1} [27]. The stretching band υ C=N is responsible for the band detected at 1616 cm^{-1} [28]. As well as the stretching band at 1562 cm^{-1} allotted to υ C=C. Finally, the stretching band at 1242 cm^{-1} was attributed to υ C-N stretching vibration [29]. Also, the spectrum for 8-Hydroxyquinoline show a band at 3479 cm^{-1} is attributable to υ O-H stretching vibration. The bands at 3182 and 3047 cm^{-1} were allotted to υ C-H aromatic stretching vibration. In addition, the band at 1600 cm^{-1} was allotted to the υ C=N stretching vibration. Finally, the υ C=C stretching vibration appears at 1577 cm^{-1} [30].

The attribution of the characteristic bands in the FT-IR spectrum for the ligand $[H_2L_1]$ and its complexes is described in Table 2. The ligand $[H_2L_1]$ contains an N-H secondary amine group at 3375 cm^{-1}, which remained in the complexes and had frequencies at 3414, 3387, 3379, 3417, and 3379, while the band at 3251 cm^{-1} in the FT-IR spectrum of the ligand $[H_2L_1]$ caused by the N-H enaminone stretching vibration indicates that the ligand is loose. Moreover, the band disappearance of the hydroxyl group at 3498 cm^{-1} in all complexes is due to the replacement of the potassium ion from potassium hydroxide in place of the hydrogen ion in the carboxyl group. As well as, the FT-IR spectra for 8-hydroxyquinoline have a band at 3479 cm^{-1} that is caused by the O-H group stretching vibration. However, on complexation, these bands disappear for complexes **1**, **2**, **3**, **4** and **5**, demonstrating that the coordination occurs through the oxygen atom of the hydroxyl group for (8-HQ) and the nitrogen atom of the enamine group for $[H_2L_1]$.

The band at 1600 cm^{-1} for the C=N of 8-hydroxyquinoline, but this band has been shifted to a lower frequency at 1604, 1608, 1600, (1600), and 1600 cm^{-1} for complexes **1**, **2**, **3**, **4**, and **5** respectively, suggesting that the coordination is via the nitrogen atom of the C=N group. Because

oxygen and nitrogen atoms are coordinated to the metal atom, the carbonyl group and the imine group have lower frequencies.

In FT-IR complexes, the appearance of new bands at 547, 586, 543, 582, 540, 563, 532, 586, and 540, 563 cm^{-1} were allotted to υ M-O for complexes **1**, **2**, **3**, **4** and **5** indicating that to the oxygen of ligands are included in coordination with metals ions. In addition, υ M-N was assigned to the appearance of new bands at 412, 447, 459, 459, 432, 459, 432, 459, and 432, 459 cm^{-1} for **1**, **2**, **3**, **4**, and **5** complexes [31-33].

At lower frequencies of the complexes, the appearance of new bands at 368, 351, 372, 351, 381, 351 and 378, 349 cm^{-1} were allotted to υ M-Cl for **1**, **2**, **4**, and complexes [33]. The FT-IR spectra for complex Cd(II) as shown in Figure S2 (Supporting information).

Table 2: FT- IR spectral data (wave number) cm^{-1} of $[H_2L_1]$, (8-HQ), K_2 $[Co(L_1)(Q)Cl_2]$ (**1**) ,$K_2[Ni(L_1)(Q)Cl_2]$ (**2**), $[Pd(L_1)(Q)]$ (**3**), $K_2[Cd(L_1)(Q)Cl_2]$ (**4**) and $[Pt(L_1)(Q)Cl_2]$ (**5**)

Compounds	$[H_2L_1]$	8-HQ	*(1)*	*(2)*	*(3)*	(4)	(5)
υ(N-H)	3375 3251	-	3414	3387	3352	3417	3379
$υ(C=O)_{carb.}$ $υ(C=O)_{dim.}$	1685 1616	- -	1604 1577	1608 1577	1708 1600	1600 1573	1708 1600
$υ(C-H)_{aliph.}$	2958 2873	-	2962 2870	2958 2889	29582893	29272854	2962 2893
$υ(C-H)_{arom.}$	3082	318230 47	3047	3047	3062	3051	3089
υ(C-N)	1242	1222	1269	1265	1234	1269	1234
υ(C=N)	1616	1600	1604	1608	1600	1600	1600
υ(C=C)	1562	1562	1465	1465	1469	1462	1469
$υ_{asy}(S=O)$ $υ_{sy}(S=O)$	1346 1165	- -	1381 1165	1377 1161	1369 1165	1384 1127	1373 1165
υ(O-H)	3498	3479	-	-	-	-	-
υ(M-N)	-	-	412447	459459	432459	432459	432459
υ(M-O)	- -	- -	547 586	543 582	540 563	532 586	540 563
υ(M-Cl)	- -	- -	368 351	372 351	- -	381 351	351 368

Nuclear magnetic resonance spectra of the ligand $[H_2L_1]$

^{1}H-NMR spectrum of the ligand $[H_2L_1]$

Figure S3 (Supporting information) represents the ^{1}H-NMR spectrum of $[H_2L_1]$. The spectrum shows the singlet signal at δ = 13.16 ppm is assigned to the O-H proton of the carboxylic acid group [34]. The singlet signal at δ = 8.6 ppm is attributed to the one proton for the N-H enamine group of S-NH, and the singlet signal at δ = 8.41 ppm is allotted to the proton for the N-H of C_8-NH secondary amine. The aromatic signals in the $[H_2L_1]$ spectra are single chemical shifts at δ=8.36ppm, δ=7.11ppm and are assigned to protons of C_4 and C_7 aromatic ring [35, 36]. Table 3 provides a summary of all of these references.

^{13}C-NMR spectrum for the precursor $[H_2L_1]$

The ^{13}C-NMR spectrum of $[H_2L_1]$. In the middle of the DMSO-d_6 solvent, as depicted in Figure S4 (Supporting information), the first carbonyl group for an aliphatic ring was detected around δ=169.09 ppm. The carbonyl group for aromatic ring observed around δ=168.82 ppm. The chemicals shift at δ=152.83 ppm and δ = 151.79 ppm allotted to C_8 for C_8-NH group and C_{16} for C_{16}-NH respectively [37, 38]. Multiples of chemical shifts at δ=133.78-110.99 ppm range are allotted to C_6, C_5, C_4, C_7 for the aromatic ring. The chemical shifts at δ= 143.17 ppm, δ= 136.66 ppm, δ= 108.62 ppm, and δ= 108.09 ppm were assigned to C_{14}, C_{11}, C_{12}, and C_{13}, respectively, for the furan ring. The chemical shift at δ= 102.90

ppm to C_3 for C_3-CO and C_{17} for C_{17}-CO. The chemical shifts at δ= 40.88 ppm were attributed to C_{10}, C_{19}, and C_{21} for the CH_2 groups. The chemical shift to DMSO solvent occurs at δ= 39.97 ppm. The chemical shift at δ= 32.58 ppm refers to C_{20} for the aliphatic ring. Finally, the carbon atoms C_{22} of CH_3 groups resonated with the chemical shifts at δ = 28.41 ppm [39, 40]. Table 4 gives a summary of the results.

Table 3: ^{1}H-NMR spectrum data for the precursor [H_2L_1]

Compound	Functional groups	δ (ppm)
[H_2L_1] 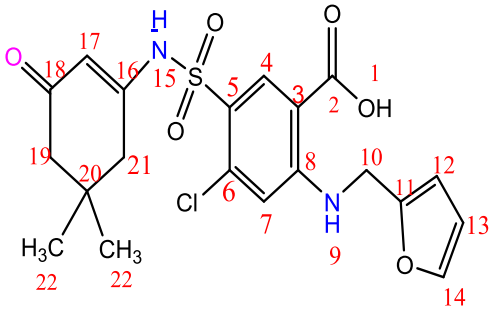	O-H carboxylic acid	13.16
	C_{16}-NH Enaminone group	8.65
	N-H For C_8–NH group	8.41
	C_4 , C_7 For Ar-H	8.36, 7.11
	C_{10} For CH_2 group	4.63
	C_{12} ,C_{13}, C_{14} For CH group of the furan	6.42, 6.38, 7.62
	C_{17} For CH group	5.21
	C_{19}, C_{21} For CH_2 groups	2.13, 2.29
	C_{22} For CH_3 groups	0.99, 1.03
	DMSO Solvent	2.5

Table 4: ^{13}C-NMR spectrum data for precursor [H_2L_1]

Compound	Functional groups	δ (ppm)
[H_2L_1] 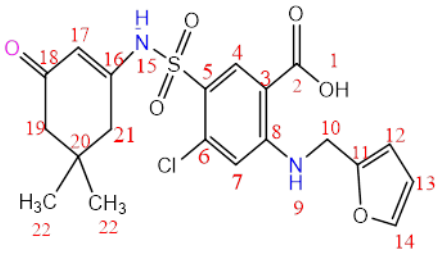	C=O for aliphatic ring	169.09
	C=O for aromatic ring	168.82
	C_8-NH for aromatic ring	152.83
	C_{16}-NH enaminone	151.79
	C_{14} for C-O of the furan ring	143.17
	C_{11} for C-O of the furan ring	136.66
	C_6 ,C_5 for aromatic ring	133.78 , 127.28
	C_4 ,C_7 for CH of the aromatic ring	114.02, 110.99
	C_{13} ,C_{12} for CH of the furan ring	108.62 , 108.09
	C_3-CO , C_{17}-CO groups	102.90
	C_{10} ,C_{19},C_{21} for CH_2 of the aliphatic ring	40.88
	C_{20} for aliphatic ring	32.58
	C_{22} for methyl groups	28.41

Mass spectrum of the precursor [H_2L_1]

Positive ESI-MS for [H_2L_1] is seen in Figure S5 (Supporting information),). No peak was visible on the spectrum at m/z = 452, which may be attributable to the parent compound's molecular ion $[M\text{-}H]^+$. While the peak appeared at 450, which could be attributed to $[M^{-2}]^+$ [41]. As well as the appearance of the peak at m /z = 407, which can be traced to $[C_{19}H_{20}ClN_2O_5S]^+$. Resulting from the fragment of the carboxyl group included in the ligand. The fragmentation pattern of [H_2L_1] is shown in Table 5.

UV-Vis spectra of ligand [H_2L_1],8-HQ, and their metal complexes

Table 6 gives the UV-Vis spectra of [H_2L_1], 8-HQ, and their complexes K_2 [Co(L_1) (Q)Cl_2] (**1**), K_2 [Ni(L_1) (Q)Cl_2] (**2**), [Pd(L_1) (Q)] (**3**), K_2 [Cd(L_1) (Q)Cl_2] (**4**) and [Pt(L_1) (Q)Cl_2] (**5**) complexes that measured in DMSO, in the range 200-1000 nm.

Figures S6 and S7 (Supporting information),) [Pt(L_1) (Q)Cl_2] complexes. Electronic spectrum of K_2 [Cd(L_1) (Q)Cl_2] and

Table 5: A Fragmentation pattern belonging to[H_2L_1]

Fragment	MASS/Charge (m/z)
$[C_{20}H_{21}ClN_2O_6S]^+$	Not detected
$[C_{19}H_{20}ClN_2O_4S]^{+\cdot}$	407
$[C_{17}H_{13}ClN_2O_5S]^{+\cdot}$	393
$[C_{14}H_{11}ClN_2O_5S]^{+\cdot}$	354
$[C_{14}H_{12}ClNO_5S]^{+\cdot}$	341
$[C_{14}H_{14}ClNO_3S]^{+\cdot}$	311
$[C_{11}H_6ClO_5S]^{+\cdot}$	285
$[C_{10}H_6ClNO_3S]^{+\cdot}$	256
$[C_{11}H_8NO_3S]^{+\cdot}$	234
$[C_{10}H_{13}NO_3S]^{+\cdot}$	227
$[C_5H_5O]^{+\cdot}$	81

Table 6: UV-Vis spectral data of [H_2L_1], 8-HQ and mixed ligand complexes in DMSO solution

Compound	*Wave number*		*ε_{max} molar^{-1}.cm^{-1}*	*Assignment*	*μ_{eff} (B.M)*	*Suggested structure*
	Nm	*cm^{-1}*				
[H_2L_1]	272 345	36764.7 28985.5	1863 1909	$\pi \rightarrow \pi^*$ $n \rightarrow \pi^*$	-	- -
8-HQ	279 324	35842.2 30864.1	2213 1232	$\pi \rightarrow \pi^*$ $n \rightarrow \pi^*$	-	- -
1	271 345 402 689 766 806	36900.3 28985.5 24875.6 14513.7 13054.8 12406.9	1774 1172 938 56 56 54	L.F L.F C.T $^4T_1g_{(F)} \rightarrow {}^4T_1g_{(P)}$ $^4T_1g_{(F)} \rightarrow {}^4A_2g_{(F)}$ $^4T_1g_{(F)} \rightarrow {}^4T_2g_{(F)}$	4.76	distorted octahedral
2	273 344 393 760 925	36630 29069.7 25445.2 13157.8 10810.8	2046 2060 1630 14 12	L.F L.F C.T $^3A_2g_{(F)} \rightarrow {}^3T_1g_{(F)}$ $^3A_2g_{(F)} \rightarrow {}^3T_2g_{(F)}$	3.08	distorted octahedral
3	270 301 348 711 797	37037 33222.5 28735.6 14064.9 12547	1557 1554 1120 22 22	L.F L.F C.T $^1A_1g \rightarrow {}^1E_1g$ $^1A_1g \rightarrow {}^1B_1g$	-	square planar
4	273 328 393	36630 30487.8 25445.2	2041 1063 591	L.F L.F C.T	-	distorted octahedral
5	269 348 363 688	37174.7 28735.6 27548.2 14534.8	1405 863 1212 19	L.F L.F C.T $^1A_1g \rightarrow {}^3T_2g$	-	distorted octahedral

*Biological activity for the ligand [H_2L_1],8-Hydroxyquinoline and their complexes $K_2[Co(L_1)(Q)Cl_2]$ (**1**), $K_2[Ni(L_1)(Q)Cl_2]$ (**2**), $[Pd(L_1)(Q)]$ (**3**), $K_2[Cd(L_1)(Q)Cl_2]$ (**4**), $[Pt(L_1)(Q)Cl_2]$ (**5**)*

The biological activity of the ligand [H_2L_1] and a number of its metal complexes **1**, **2**, **3**, **4**, and **5**, were tested for their antibacterial activity against Staphylococcus *aureus* which is a Gram-positive bacterium, and *Escherichia coli*, which is a Gram-negative bacterium, as well as the fungi (*Candida albicans*).

The following conclusions are drawn from the information recorded and displayed in the Table 7.

Using the concentration (10^{-2}M):

Escherichia coli: The ligand [H_2L_1] and the complex **3** displayed similar activity in inhibiting *Escherichia coli* compared to the rest of the complexes. At varying rates, the complexes inhibited testing bacteria, with **3** >**2** >**1**>**4** = **5** being the sequence of decreasing activity.

Staphylococcus aureus: The complex **2** showed higher activity in inhibiting Staphylococcus aurous than the rest of the same ligand complexes and the ligand [H_2L_1]. The Complexes inhibited testing bacteria at varied rates, with **2** > **3** = **4** > **5** > **1** the order of decreasing activity being. Complex **1** showed similar inhibition to the ligand [H_2L_1].

Candida albicans: The complex 3 offered a higher activity in inhibiting *Candida albicans than* the rest of the same ligand complexes and the ligand [H_2L_1]. The complexes inhibited testing the fungi at varied rates, with **3** > **1** > **2** > **5** > **4** the order of decreasing activity. For information, Complex **4** showed less inhibitory activity than the ligand [H_2L_1]. Figures 1, 2 and 3 show the biological activity of [H_2L_1] and its complexes on *Escherichia Coli, Staphylococcus aureus and Candida albicans* at concentration of 10^{-2}M.

Utilizing the concentration (10^{-3}M)

Escherichia coli: The ligand [H_2L_1] revealed higher activity in inhibiting *Escherichia coli* than their complexes. The Complexes inhibited tested bacteria at varying rates, with **1** = **5** >**3** = **4** >**2** being the sequence of decreasing activity. Complexes 2 and 3 and 4 showed less inhibitory activity than the ligand [H_2L_1].

Staphylococcus aureus: The complex **1** displayed higher activity in inhibiting of *Staphylococcus aureus* than the rest of the same ligand complexes and the ligand [H_2L_1]. At varying rates, the Complexes inhibited testing bacteria, with **1** > **2**= **3** = **4** > **5** the order of decreasing activity.

Candida albicans: The ligand [H_2L_1] and the complex **1**, **3**, and **4** displayed similar activity inhibiting *Candida albicans*. The Complexes inhibited testing the fungi at varied rates, with **1** = **3** = **4** > **2** > **5** the order of decreasing activity.

Some complexes are inhibiting because of the increased lipophilicity of the complexes. Overton and Chelation's theory could explain this increased activity of metal complexes. The positive charge of the metal in the chelated complex is partially probably shared with the ligand donor atoms, resulting in electron delocalization throughout the entire chelate ring. This, enhances the lipophilicity of the metal chelate and facilitates its passage via the lipoid layers of bacterial membranes [42]. Figures 4, 5 and 6 show the biological activity of [H_2L_1] and its complexes on Escherichia Coli, Staphylococcus aureus and Candida albicans at concentration of (10-3M). Figures 7 and 8 illustrate Evolution of [H_2L_1] and its complexes against *Escherichia Coli, Staphylococcus aureus* and *Candida albicans* growth at concentrations 10^{-2}M and 10^{-3} M.

Table 7: Inhibition zone diameter in (mm) for the ligand [H_2L_1]and their complexes

Compounds	*Escherichia coli*		*Staphylococcus aureus*		*Candida albicans*	
	10^{-2} M	10^{-3} M	10^{-2} M	10^{-3} M	10^{-2} M	10^{-3} M
[H_2L_1]	19	21	12	16	15	20
Anti	22	22	21	21	21	21
1	16	17	12	18	23	20
2	18	13	20	17	21	18
3	19	15	16	17	26	20
4	15	15	16	17	14	20
5	15	17	15	16	15	17

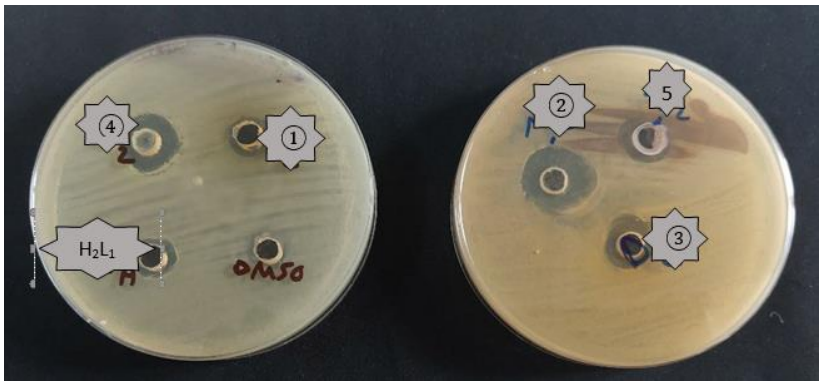

Figure 1: The biological activity (*Staphylococcus auras*) of the mixed-ligand complexes K_2 [$Co(L_1)(Q)Cl_2$] (**1**), $K_2[Ni(L_1)(Q)Cl_2)]$ (**2**), [$Pd(L_1)(Q)$] (**3**), $K_2[Cd(L_1)(Q)Cl_2)]$ (**4**) ,[$Pt(L_1)(Q)Cl_2$] (**5**) at concentration 10^{-2}M

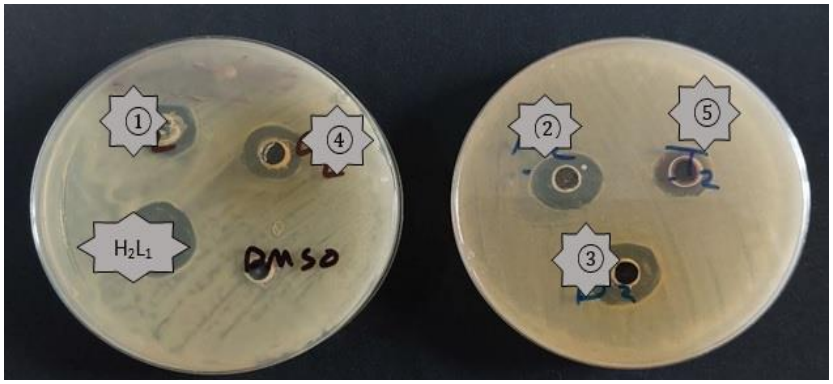

Figure 2: The biological activity (*Escherichia coli*) of the mixed-ligand complexes K_2 [$Co(L_1)(Q)Cl_2$] (**1**), $K_2[Ni(L_1)(Q)Cl_2)]$ (**2**),[$Pd(L_1)(Q)$] (**3**), $K_2[Cd(L_1)(Q)Cl_2)]$ (**4**), [$Pt(L_1)(Q)Cl_2$] (**5**) at concentration 10^{-2}M

Figure 3: The biological activity *(candida albicans)* of the mixed-ligand complexes K_2 [$Co(L_1)(Q)Cl_2$] (**1**), $K_2[Ni(L_1)(Q)Cl_2)]$ (**2**),[$Pd(L_1)(Q)$] (**3**), $K_2[Cd(L_1)(Q)Cl_2)]$ (**4**), [$Pt(L_1)(Q)Cl_2$] (**5**) at concentration 10^{-2} M

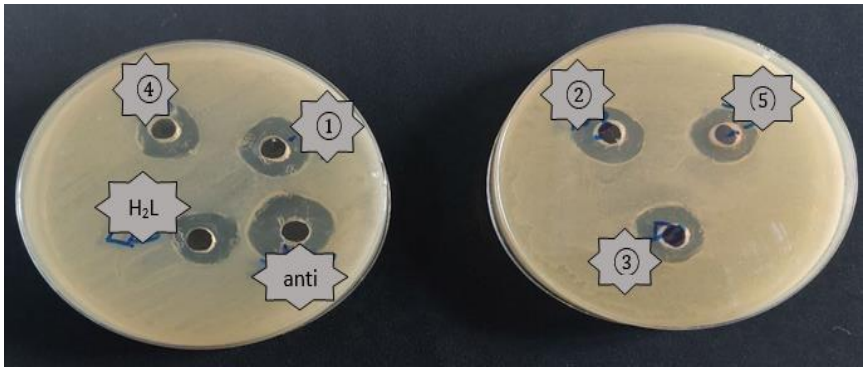

Figure 4: The biological activity *(Staphylococcus auras)* of the mixed-ligand complexes K_2 [$Co(L_1)(Q)Cl_2$] (**1**), $K_2[Ni(L_1)(Q)Cl_2)]$ (**2**),[$Pd(L_1)(Q)$] (**3**), $K_2[Cd(L_1)(Q)Cl_2)]$ (**4**), [$Pt(L_1)(Q)Cl_2$] (**5**) at concentration 10^{-3}M

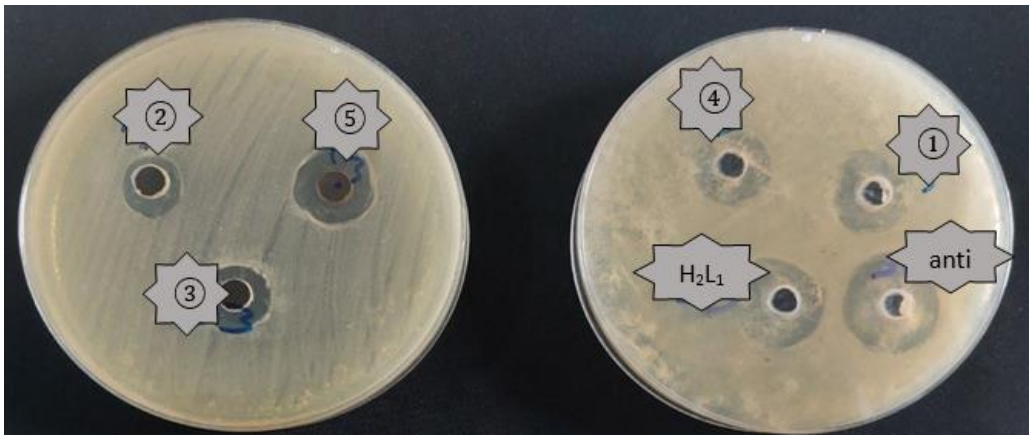

Figure 5: The biological activity (*Escherichia coli*) of the mixed-ligand complexes where K_2 [$Co(L_1)(Q)Cl_2$] (**1**), $K_2[Ni(L_1)(Q)Cl_2)]$ (**2**),[$Pd(L_1)(Q)$] (**3**), $K_2[Cd(L_1)(Q)Cl_2)]$ (**4**), [$Pt(L_1)(Q)Cl_2$] (**5**) at concentration 10^{-3}M

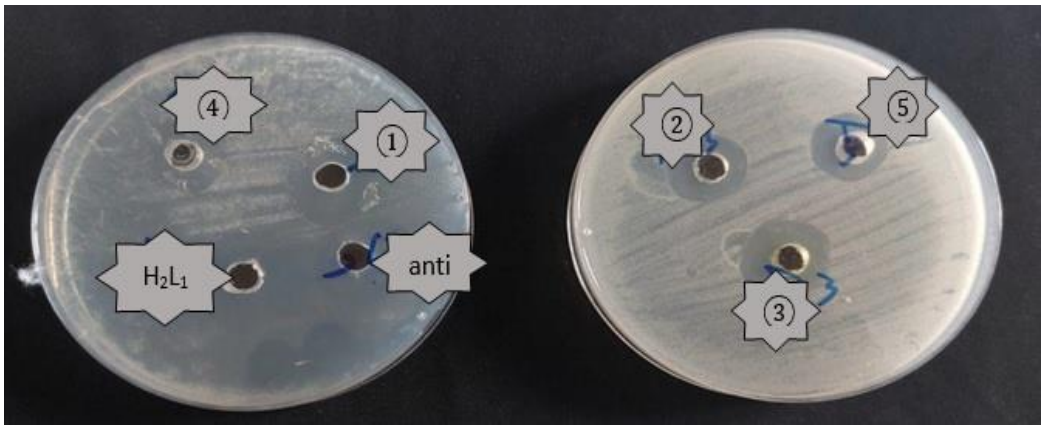

Figure 6: The biological activity (*candida albicans*) of the mixed-ligand complexes K_2 [$Co(L_1)(Q)Cl_2$] (**1**), $K_2[Ni(L_1)(Q)Cl_2)]$ (**2**),[$Pd(L_1)(Q)$] (**3**), $K_2[Cd(L_1)(Q)Cl_2)]$ (**4**), [$Pt(L_1)(Q)Cl_2$] (**5**) at concentration 10^{-3}M

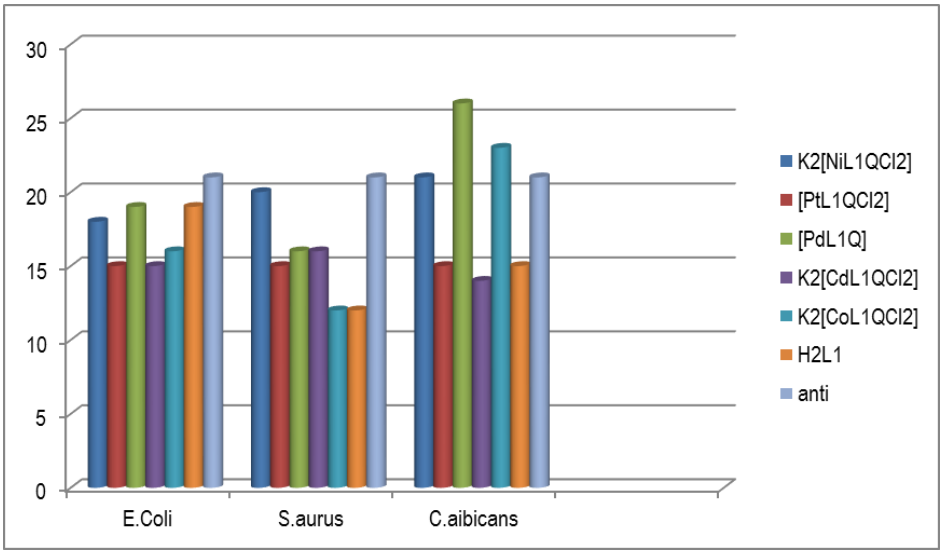

Figure 7: Evolution of [H_2L_1] and its complexes against *Candida albicans, E. coli* and *S. aureus* growth at concentration 10^{-2}M

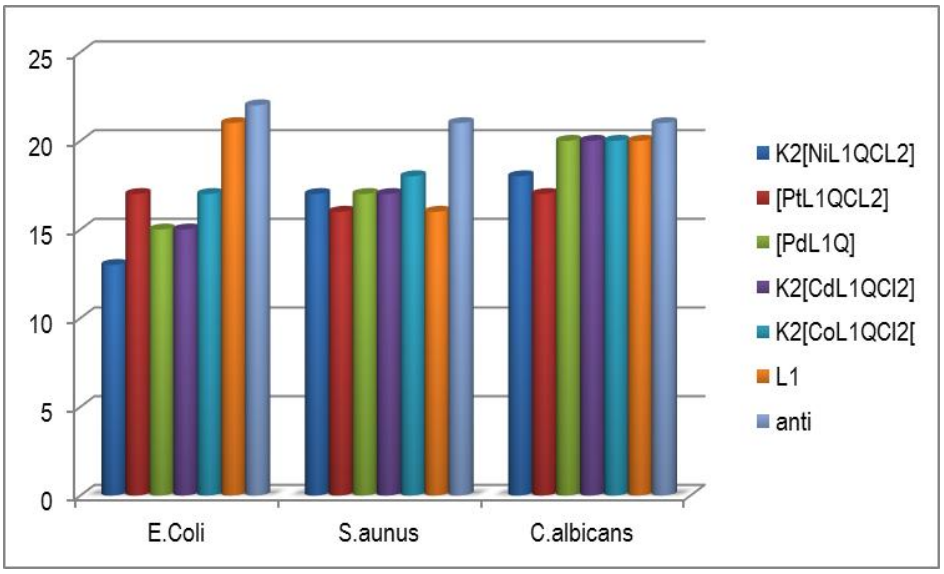

Figure 8: Evolution of [H_2L_1] and its complexes *a*gainst *Candida albicans, E. coli and S. aureus* growth at concentration 10^{-3} M

Conclusion

1-The *β*-enaminone acted in the form of bidentate ligand through a nitrogen atom in imine (N-H) and oxygen atom in (C=O) $_{keto}$. with the central metal ions M(II): Co, Ni, Pd, Cd also Pt (IIII) with complexes of its general molecular formula: [M (L_1) (Q) Cl_2] and complexes [Pd (L_1) (Q)] and [Pt(L_1) (Q)Cl_2]. 2-For all prepared complexes Co(II), Ni(II), Cd(II), Pt(IIII), the octahedral geometrical structure was recommended while Pd(II) the Square planar geometrical.

Acknowledgments

Thanks, and appreciation to the presidency of the University of Baghdad and to the Deanship of the College of Education for Pure Sciences Ibn Al-Haitham and everyone who contributed to this research.

Funding

This research did not receive any specific grant from funding agencies in the public, commercial, or not-for-profit sectors.

Authors' contributions

All authors contributed to data analysis, drafting, and revising of the paper and agreed to be responsible for all the aspects of this work.

Conflict of Interest

There are no conflicts of interest in this study.

Supporting Information

The Supporting Information is available free of charge at http://www.chemmethod.com/article_156750.html
Detailed spectra of synthesized compounds (PDF)

References

[1]. Shashikanth J., Shashank M., Sumedha H.N., Alharthi F.A., Nizam A., Reddy M., Nagaraju G., Tamarindusindica Mediated Combustion Synthesis of BiOCl: Photocatalytic Degradation of Dyes and Synthesis of β-Enaminones, *Journal of Electronic Materials*, 2021, **50**:4650 [Crossref], [Google Scholar], [Publisher]

[2]. 2-Khanikar S., Kaping S., Helissey P., Joshi P., Shaham S.H., Mishra S., Srivastava M., Tripathi R., Vishwakarma J.N., Efficient synthesis, structure elucidation, and anti-parasitic activities of novel quinolinyl β–enaminones, *Monatshefte Fur Chemie*, 2021, **152**:665 [Crossref], [Google Scholar], [Publisher]

[3]. Prabakaran K., Sivakumar M., Perumal M.S., A Simple, Efficient Green Protocol for the Synthesis of β-Enaminone and Enamino Ester Derivatives by Using Onion Extract as Green

Catalyst, *ChemistrySelect*, 2017, **2**:2363 [Crossref], [Google Scholar], [Publisher]

[4]. Shashikanth J., Shashank M., Sumedha H.N., Alharthi F.A., Nizam A., Reddy M., Nagaraju G., Tamarindusindica Mediated Combustion Synthesis of BiOCl: Photocatalytic Degradation of Dyes and Synthesis of β-Enaminones, *Journal of Electronic Materials*, 2021, **50**:4650 [Crossref], [Google Scholar], [Publisher]

[5]. Chniti S., Nsira A., Khouaja S., Mechria A., Gharbi R., Msaddek M., Lecouvey M., Highly diastereoselective synthesis of rigid 3-enamino-1, 5-benzodiazepines, *Arkivoc*, 2018, **2018**:283 [Crossref], [Google Scholar], [Publisher]

[6]. Mohareb R.M., Manhi F.M., Mahmoud M.A.A., Abdelwahab A., Uses of dimedone to synthesis pyrazole, isoxazole and thiophene derivatives with antiproliferative, tyrosine kinase and Pim-1 kinase inhibitions, *Medicinal Chemistry Research*, 2020, **29**:1536 [Crossref], [Google Scholar], [Publisher]

[7]. Nikoofar K., Yielzoleh F.M., A concise study on dimedone: A versatile molecule in multi-component reactions, an outlook to the green reaction media, *Journal of Saudi Chemical Society*, 2018, **22**:715 [Crossref], [Google Scholar], [Publisher]

[8]. Rao T.N., Krishnarao N., Ahmed F., Alomar S.Y., Albalawi F., Mani P., Aljaafari A., Parvatamma B., Arshi N., Kumar S., One-pot synthesis of 7, 7-dimethyl-4-phenyl-2-thioxo-2,3,4,6,7, 8-hexahydro-1H-quinazoline-5-onesusing zinc ferrite nanocatalyst and its bio evaluation, *Catalysts*, 2021, **11**:431 [Crossref], [Google Scholar], [Publisher]

[9]. Karabulut S., Namli H., Leszczynski J., Detection of tautomer proportions of dimedone in solution: A new approach based on theoretical and FT-IR viewpoint, *Journal of Computer-Aided Molecular Design*, 2013, **27**:681 [Crossref], [Google Scholar], [Publisher]

[10].Hassouna M.E., Issa Y.M., Zayed A.G.,' Spectrophotometric Determination of Furosemide Drug in Different Formulations using Schiff 's Bases, *Foresic Research & Criminology International Journal*, 2016, **1**:00036 [Crossref], [Google Scholar], [Publisher]

[11].McMahon B.A., Chawla L.S., The furosemide stress test: current use and future potential, *Renal Failure*, 2021, **43**:830 [Crossref], [Google Scholar], [Publisher]

[12].Saleem B.A.A., Hamdon E.A., Majeed S.Y., Visible Quantitative Methods for the Estimation of Furosemide in Pure form and Pharmaceutical Formulations, *Journal of Pharmaceutical Research International*, 2021, 200 [Crossref], [Google Scholar], [Publisher]

[13].Vlachou M., Geraniou E., Siamidi A., Modified release of furosemide from Eudragits and poly(ethylene oxide)-based matrices and dry-coated tablets. *Acta Pharmaceutica*, 2020, **70**:49 [Crossref], [Google Scholar], [Publisher]

[14].Vlachou M., Pippa N., Siamidi A., Kyrili A., Thermal analysis studies on the compatibility of furosemide with solid state and liquid crystalline excipients, *Hemijska Industrija*, 2020, **74**:15 [Crossref], [Google Scholar], [Publisher]

[15].Kerr H.E., Softley L.K., Suresh K., Nangia A., Hodgkinson P., Evans I.R., A furosemide-isonicotinamide cocrystal: An investigation of properties and extensive structural disorder, *CrystEngComm*, 2015, **17**:6707 [Crossref], [Google Scholar], [Publisher]

[16].Obaid S.M.H., Jarad A.J., Salih Al-Hamdani A.A., Synthesis, Characterization and Biological Activity of Mixed Ligand Metal Salts Complexes with Various Ligands, *Journal of Physics: Conference Series*, 2020, **1660**:012028 [Crossref], [Google Scholar], [Publisher]

[17].Patil S.S., Langi B.P., Gurav M.N., Patil D.K., Synthesis, Physical and Spectral Investigations and Biological Studies of Mixed Ligand Lanthanum Complexes, *Annals of the Romanian Society for Cell Biology*, 2021, **25**:10559 [Google Scholar], [Publisher]

[18].Akter J., Hanif A., Islam S., Reza, Haque M., Zahid, M., Zahan K.E., Islam A., Banu L.A., Mixed Ligand Complexes of Ni(II) And Cd(II) With Phthalic Acid Orsuccinic Acid And Heterocyclic Amines: Synthesis Andcharacterization With Antimicrobial Study, *European Journal Of Pharmaceuticaland Medical Research*, 2018, **5**:106 [Google Scholar], [Publisher]

[19].Nesa S., Hossain S., Nasira S., Uddin N., Ashrafuzzaman M., Habib A., Rashid A.M., Haque

M., Mixed ligand complexes: Synthesis, characterization and antibacterial activity investigation, *International Journal of Chemical Studies*, 2020, **8**:306 [Crossref], [Google Scholar], [Publisher]

[20].Saritha A., Reddy C.V.R., Sireesha B., Synthesis, characterization and biological activity of mixed ligand chelates of Ni(II) with pyridoxalthiosemicarbazone and dipeptides, *Vietnam Journal of Chemistry*, 2021, **59**:57 [Crossref], [Google Scholar], [Publisher]

[21].Nan P., Xia X., Du, Q., Chen J., Wu X., Chang Z., Genotoxic effects of 8-hydroxylquinoline in loach (Misgurnus anguillicaudatus) assessed by the micronucleus test, comet assay and RAPD analysis, *Environmental Toxicology and Pharmacology*, 2013, **35**:434 [Crossref], [Google Scholar], [Publisher]

[22].Mohammed S., Obaid H., Mahdi W., Hussein F.H., Al-Khafaji Y., Recent Development In Oxine Complexes And Their Medical Application: A Review, *Systematic Reviews in Pharmacy*, 2020, **11**:428 [Google Scholar], [Publisher]

[23].Southcott L., Wang X., Wharton L., Yang H., Radchenko V., Kubeil M., Stephan H., de Guadalupe Jaraquemada-Peláez M., Orvig C., High denticity oxinate-linear-backbone chelating ligand for diagnostic radiometal ions [111In]In3+ and [89Zr]Zr4+, *Dalton Transactions*, 2021, **50**:3874 [Crossref], [Google Scholar], [Publisher]

[24].Southcott L., Orvig C., Inorganic radiopharmaceutical chemistry of oxine, *Dalton Transactions*, 2021, **50**:16451 [Crossref], [Google Scholar], [Publisher]

[25].Shashikanth J., Shashank M., Sumedha H.N., Alharthi F.A., Nizam A., Reddy M., Nagaraju G., Tamarindusindica Mediated Combustion Synthesis of BiOCl: Photocatalytic Degradation of Dyes and Synthesis of β-Enaminones, *Journal of Electronic Materials*, 2021, **50**:4650 [Crossref], [Google Scholar], [Publisher]

[26].Kadhom H.J., Numan A.T., Atiyah E.M., Characterization of New Ligand for β-enaminone and its Mixed Ligand Complexes with Some Metal Ions and Evaluation of their Biological Activity Synthesis and Characterization of New Ligand for β-enaminone and its Mixed Ligand Complexes with Some Metal Ions and Evaluation of their Biological Activity, *International Journal of Drug Delivery Technology*, 2022, **12**:640 [Crossref], [Google Scholar]

[27].Rashed N.M., Abdullaha S.A.H., Metal complexes of mixed ligands novel 2-Thioxoimidazolidine-4- one derivative and glycine Synthesis, characterization and biological activity, *Eurasian Journal of Physics, Chemistry and Mathematics,* 2021, **1**:29 [Google Scholar], [Publisher]

[28].SA O., Ige S.E., Synthesis, Characterization and Antimicrobial Properties of Mixed Ligand of Sulphamethoxazole and Trimethoprim and Their Manganese (II) and Copper (II) Complexes, *International Journal of Innovative Science and Research Technology,* 2022, **7** [Google Scholar], [Publisher]

[29].Nashaan F.A., Al-Rawi M.S., Alhammer A.H., Rabie A.M., Tomma J.H., Synthesis, characterization, and cytotoxic activity of some imides from galloyl hydrazide, *Eurasian Chemical Communications*, 2022, **4**:966 [Crossref], [Google Scholar], [Publisher]

[30].Fadel Z.H., Al-Azzawi A.M., Design, Synthesis and Antimicrobial Activity Evaluation of New Bisimidyl Sulfonamido Ketone Comprising Drug component, *Chemical Methodologies*, 2021, **5**:464 [Crossref], [Google Scholar], [Publisher]

[31].Ismael M., Abdel-Mawgoud A.M.M., Rabia M.K., Abdou A., Ni(II) mixed-ligand chelates based on 2-hydroxy-1-naphthaldehyde as antimicrobial agents: Synthesis, characterization, and molecular modeling, *Journal of Molecular Liquids*, 2021, **330**:115611 [Crossref], [Google Scholar], [Publisher]

[32].Al-Farhan B.S., Basha M.T., Abdel Rahman L.H., El-Saghier A.M.M., El-Ezz D.A., Marzouk A.A., Shehata M.R., Abdalla E.M., Synthesis, dft calculations, antiproliferative, bactericidal activity and molecular docking of novel mixed-ligand salen/8-hydroxyquinoline metal complexes, *Molecules*, 2021, **26**:4725 [Crossref], [Google Scholar], [Publisher]

[33].Ali F.M., Ahmed H.M., Synthesis of Pectin Graft Drug to Treatment the Wounds and Inflammations, *Chemical Methodologies*, 2019, **3**:670 [Crossref], [Google Scholar], [Publisher]

[34].Nagesh G.Y., Mruthyunjayaswamy B.H.M., Synthesis, characterization and biological relevance of some metal (II) complexes with oxygen, nitrogen and oxygen (ONO) donor Schiff base ligand derived from thiazole and 2-hydroxy-1-naphthaldehyde, *Journal of Molecular Structure*, 2015, **1085**:198 [Crossref], [Google Scholar], [Publisher]

[35].Uttu A.J., Sallau M.S., Iyun O.R.A., Ibrahim H., ''Isolation, Characterization and In Silico Molecular Docking Studies of Two Terpenoids from Strychnos innocua (Delile) Root Bark for Antibacterial Properties'', *Advanced Journal of Chemistry-Section A*, 2022, **5**:241 [Crossref], [Google Scholar], [Publisher]

[36].Chniti S., Nsira A., Khouaja S., Mechria A., Gharbi R., Msaddek M., Lecouvey M., Highly diastereoselective synthesis of rigid 3-enamino-1, 5-benzodiazepines, *Arkivoc*, 2018, **2018**:283 [Crossref], [Google Scholar], [Publisher]

[37].Abdulghani S.M., Al-Rawi S., Tomma J.H., Chemical Methodologies Synthesis of New 1,2,4-Triazole Derivatives with Expected Biological Activities, *Chemical Methodologies*, 2022, **6**:59 [Crossref], [Google Scholar], [Publisher]

[38].Mansour S.T., Hashem A.I., Abd-El-Maksoud M.A., El-Hussieny M., El-Makawy A.I., Abdel-Aziem S.H., Soliman F.M., The synthesis and antineoplastic activities of thiaziridine, sulfidometylphosphonium, and dithiaphosphitane-sulfide against the Ehrlich ascites carcinoma. Fundamental and Clinical Pharmacology, 2022, **36**:536 [Crossref], [Google Scholar], [Publisher]

[39]. Onyenze U., Edozie O.I., Synthesis, Spectroscopic Characterization and Antibactrial Activities of Co(II) Complex of ofloxacin Drug Mixed with Ascorbic Acid as a Secondary Ligand Synthesis, Spectroscopic Characterization and Antibacterial Activities of Co(II) Complex of Ofloxacin Drug Mixed with Ascorbic Acid as Secondary Ligand, *BioScientific Review*, 2021, **3**:1 [Crossref], [Google Scholar], [Publisher]

[40].Al-Jeilawi O.H.R., Khudhair N.A., Chemical Methodologies Novel Synthesis of Some N-Hydroxy Phthalimide Derivatives with Investigation of Its Corrosion Inhibition for Carbon Steel in HCl Solution, *Chemical Methodologies*, 2021, **5**:331 [Crossref], [Google Scholar], [Publisher]

[41].Patil S.S., Tadavi S.K., Dikundwar A., Bendre R.S., The transition metal complexes of Fe(II), Ni(II) and Cu(II) derived from phthalazine based ligands: Synthesis, crystal structures and biological activities, *Journal of Molecular Structure*, 2022, **1247**:131293 [Crossref], [Google Scholar], [Publisher]

[42].Hamad B.K., Ahamed M.R., "Synthesis of new compounds with seven rings (oxazepine) through the ring closure of Schiff bases with study of biological activity", *Eurasian Chemical Communications*, 2022, **4**:1306 [Crossref], [Google Scholar], [Publisher]

HOW TO CITE THIS ARTICLE

Maysam B. Abdulsalam, Ahmed T. Numan. Synthesis, Characterization, and Biological Activity of Mixed ligand Complexes from 8-Hydroxyquinoline and New ligand for *β*-Enaminone. *Chem. Methodol.*, 2022, 6(12) 962-976
https://doi.org/10.22034/CHEMM.2022.356340.1593
URL: http://www.chemmethod.com/article_156750.html